A Preliminary Analysis of the Effect of the Onset Flow Structure on Tidal Turbine Blade Loads

I. A. Milne, R. N. Sharma, R.G.J. Flay and S. Bickerton
The University of Auckland
20 Symonds Street
Auckland, 1010 New Zealand

Abstract- **A significant challenge designers of tidal stream turbines face is ensuring that the device can survive the harsh operating environment. Understanding the effect of the onset flow structure on the loading spectrum of the blades will lead to improved blade designs. The results of a preliminary parametric analysis suggest that the mean flow speed, longitudinal turbulence intensity, wave state and depth of hub relative to the channel depth are dominant drivers of the blade loads for horizontal-axis tidal turbines. They should therefore be accurately modeled in both fatigue and extreme load analyses.**

I. INTRODUCTION

The ocean's tidal streams are an attractive and relatively un-utilized source of renewable energy. In recent years considerable development of the tidal stream turbine industry has been observed. A plethora of devices have been proposed, a number of which are now being tested at full scale [1].

However, the harsh, unsteady flow poses significant challenges for turbine developers as they attempt to ensure that a service life of at least 20 years is met. Critical components of horizontal axis type devices are the blades, which experience a high number of cycles of variable amplitude and frequency, and are commonly manufactured from composite materials. Since the fatigue life of composites is very sensitive to the loading spectrum, errors in characterizing the loads can result in premature failures. To minimize such a risk there are reports of turbine designers over-engineering the blades, in some cases by up to 30 percent [2], adding considerable cost to the device. Obviously, gaining confidence in the blade loading spectrum is critical if the blades are to be optimized.

In 2007, McCann [3] performed a parametric analysis on a generic 2MW horizontal axis, variable speed tidal turbine to investigate the effect of the turbulence intensity and wave state, and found that the blade root fatigue loads were very sensitive to both. A year later, McCann et al. [4] used site specific data from the European Marine Energy Centre (EMEC) [5] to again demonstrate the importance of understanding the nature of the turbulence intensity and waves on the blade loads. Their work also provides useful measurements of the likely structure of the onset flow structure at a tidal stream energy generation site, in terms of the turbulence intensity, shear profile and wave state. Using both numerical models and experimental testing of a scale turbine, Barltrop et al. [6] have also shown that increasing the wave period leads to greater root bending moments. However, additional literature pertaining to the characterization of tidal turbine unsteady hydrodynamic loads and the relative effect of site parameters is scarce.

This paper attempts to provide further insight into the dominant hydrodynamic drivers of the tidal turbine blade loads. The analyses consider not only the sensitivity of the blade loads to the turbulence intensity and waves, but also the sensitivity to the magnitude of the horizontal mean flow and its distribution, vertical shear profile, yaw angle, turbulence length scales, and hub height relative to the channel depth. A 500kW horizontal axis tidal turbine is used in the analyses, which is considered to be representative of the size of devices currently being designed. Where appropriate, comparisons are made against wind turbine blade loads, for which considerable knowledge now exists.

II. NUMERICAL MODELING

A. GH Tidal Bladed

The analyses presented in this paper have been performed using the commercially available software *Tidal Bladed* by Garrad Hassan [7]. *Tidal Bladed* is able to simulate the blade load response in the time domain, allowing for complex and non-linear interactions between the flow, structural dynamics, and the control system. It is an adaption of the software *Bladed* for wind turbines, and has undergone its own validation study [8].

The hydrodynamic modeling that forms the basis of *Tidal Bladed* is a combination of blade element and dynamic inflow theory. The dynamic inflow model is based on the work of Pitt and Peters [9] which introduces a time dependent apparent mass into the momentum equation. It therefore accounts for the time it takes for changes at the rotor plane to build up in the wake. The three dimensional turbulent flow-field encompasses the rotor plane and is generated by *Tidal Bladed* in normalized form, as unit-variance deviations from the mean velocity. The turbulence intensity can be therefore be adjusted separately by scaling the deviations.

B. Wave Modeling

In lieu of an inbuilt model for wave-current interaction for irregular waves in *Tidal Bladed*, a program has been written

978-1-4244-5222-4/10/$26.00 ©2010 IEEE

by the authors in Matlab to create the relevant velocity time history, which is then input back into *Tidal Bladed*. The wave kinematics are modeled using linear wave theory and the wave-current interaction is considered to cause a shift between the observed and apparent wave frequencies, while the wave height remains constant as per ISO 19901-1 [10]. The wave height spectrum conforms to the JOint North Sea WAve Project (JONSWAP) model given by Goda [11] and the superposition method is utilized to synthesize the irregular wave train. With this method, the horizontal u and vertical w wave induced velocities observed at a fixed horizontal location x and distance z below the mean water surface at time t can be expressed as

$$u(t,x,z)=\sum_{n=1}^{N} c_n \omega_{in} \frac{\cosh[k_n(z+d)]}{\sinh(k_n d)} \cos(k_n x-\omega_n-\varphi_n) \quad (1)$$

$$w(t,x,z)=\sum_{n=1}^{N} c_n \omega_{in} \frac{\sinh[k_n(z+d)]}{\sinh(k_n d)} \sin(k_n x-\omega_n-\varphi_n), \quad (2)$$

where d is the depth of the channel, located at $z=-d$, k_n ($=2\pi/L_n$) is the wave-number and L_n is the wave-length, ω_{in} ($=2\pi/T_{in}$) is the intrinsic angular frequency and T_{in} the intrinsic wave period, ω_n ($=2\pi/T_n$) is the observed angular frequency and T_n the observed wave period. The amplitude is computed from $c_n=\sqrt{a_n^2+b_n^2}$ and phase $\varphi_n = \tan^{-1}(b_n/a_n)$, where a_n and b_n are independent random variables distributed normally around zero with the standard deviation $\sigma_n = \sqrt{S(\omega_{in})d\omega_{in}}$, as discussed by Morooka and Yokoo [12]. $S(\omega_{in})$ is the wave spectral density. Wheeler stretching [13] is also employed, such that the kinematics are adjusted to the instantaneous free surface.

The observed and intrinsic wave angular frequencies are related through the Doppler shift,

$$\omega_n = \omega_{in} + k_n U \quad (3)$$

where U is the depth averaged mean flow velocity in line with the wave train. The intrinsic angular wave frequency is related to the wave number through the dispersion equation, which is expressed as,

$$\omega_{in}^2 = g k_n \tanh(k_n d) \quad (4)$$

For the cases analyzed where there is combined turbulence and waves, the wave velocity time history is superimposed on the turbulence velocity time history created internally in *Tidal Bladed*.

III. Turbine Specifications

The turbine incorporates a single horizontal-axis tri-bladed rotor which rotates at a constant speed of 15.5 RPM. Constant speed turbines have an advantage over variable speed devices in that they do not require a frequency inverter.

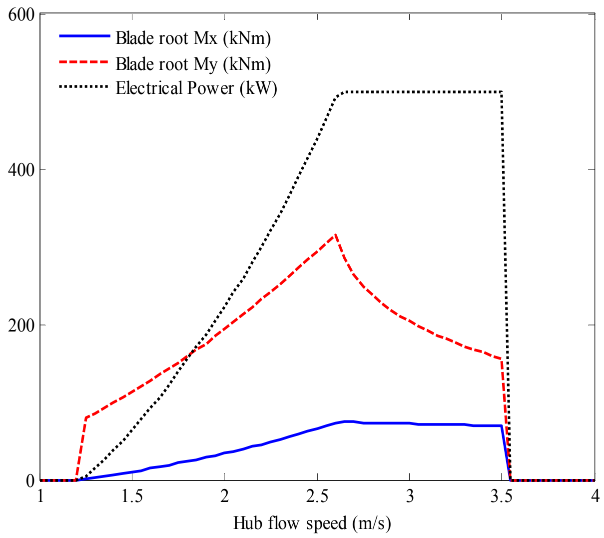

Figure 1. Blade root bending moments and turbine electrical power for a steady flow speed

However, since constant speed machines only operate at maximum efficiency for one flow speed, the device loading can be more severe.

The 6.25m long blades are based on those designed by UK tidal turbine developer, Tidal Generation Limited [14] who are currently performing full scale testing of their device. The chord, twist and thickness distribution is non-uniform, with a maximum chord of approximately 1.8m near the root and the twist varying from 35° at the root to 10° at the tip, with reference to the in-plane direction. In this study the sectional profiles conform to the NACA 44XX series, with the thickness varying from approximately 35 to 15 percent of the chord. These airfoils were successfully used for Marine Current Limited's *SeaFlow* turbine blades [15] and were also recommended as being suitable for tidal turbines by Myers [16], in an investigation into the operational characteristics of tidal turbines.

Since only limited airfoil data exists for thick sections the two dimensional airfoil properties were obtained numerically using XFOIL [17], which employs a linear vorticity stream function panel method. Previous researchers have compared the XFOIL lift and drag predictions for NACA 4415 section with published data [18]. Generally good agreement has been found for the lift coefficient prior to stall, though the magnitude of the predicted drag coefficient is lower than what has been measured experimentally.

The turbine operational characteristics in a steady, uniform flow are presented in Fig. 1. The cut-in onset flow speed is approximately 1.2m/s and rated power is obtained at approximately 2.6m/s. The dominance of the root out-of-plane bending moment M_y over that of the in-plane moment M_x can also be observed. The device is assumed to be standalone and blockage is not considered.

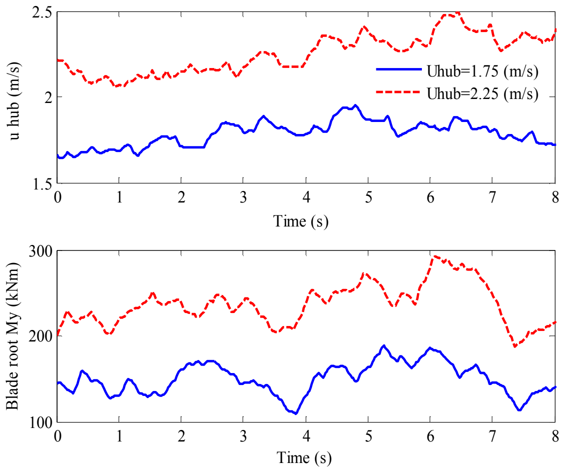

Figure 2. Time history of u measured at the hub and corresponding blade root M_y, as a function of two mean flow speeds. TI_u=7.5%

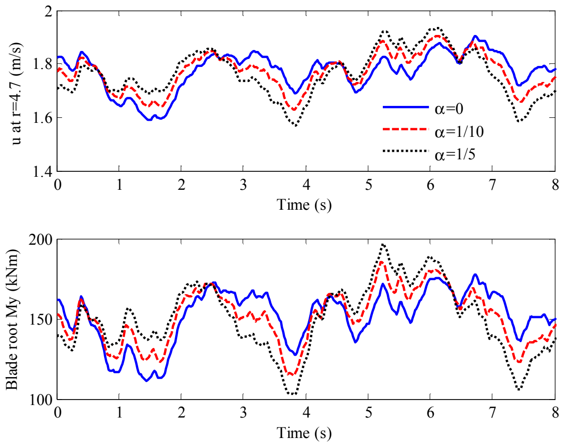

Figure 3. Time history of u as observed by the rotating blade and corresponding blade root M_y, as a function of α, for U_{hub}=1.75m/s. TI_u=7.5%

IV. Parameters Analyzed

A. *Mean hub-height velocity*

The first onset flow constituent considered is that of the longitudinal mean velocity at hub-height. Two values are considered: U_{hub}=1.75m/s and 2.25m/s. Referring to Fig. 1, at these velocities the turbine is generally operating in the below-rated region. These hub-height flow speeds are also considered representative of those which a typical tidal turbine would operate in, and are equivalent to surface velocities of 1.93m/s and 2.48m/s respectively, assuming a hub height of z_{hub}=15m above the seabed and, as discussed below, a $1/7^{th}$ vertical shear power law. An example of the hub height variation in flow speed and the corresponding root out-of-plane bending moment, as a function of time, is shown in Fig. 2.

B. *Vertical shear*

The non-uniform profile arises from the seabed imparting a shear force on the flow. During one revolution the blades will experience a variation in the mean onset velocity and therefore the magnitude of the turbulent fluctuations. Although it is only an approximation, a power law is commonly used to describe the vertical shear profile, which can be expressed as

$$\frac{u(z)}{u_{zref}} = \left[\frac{z}{z_{ref}}\right]^{\alpha}. \tag{5}$$

The exponent α is often assumed to be equal to 1/7. However as McCann et al. [4] showed, it can vary between sites, with a more severe profile which closely correlated to α=1/5 measured at EMEC. Noting this, four shear profiles have been considered for this analysis defined by α=0, 1/10, 1/7 and 1/5.

The effect of the shear profile on both the horizontal velocity observed by the blade and the corresponding variation in root bending moments can be inferred from Fig. 3. The effect of rotational sampling can also be observed, whereby the velocity fluctuation incident on the rotating blade section is greater than that observed at the hub. This is due to the rotor slicing through multiple eddies during one revolution, contributing significantly to the unsteady loads.

C. *Yaw angle*

While many tidal streams are assumed bi-directional, this is not the case at all sites. The ebb and flood tidal streams in such locations as the Cook Strait in New Zealand and Hudson Strait in Canada differ in direction by around 25°, while the Portland Bill in the UK experiences an extreme 35° shift [19]. Tidal turbines which incorporate a yaw degree of freedom can realign the rotor plane with the mean flow, however there are examples of proposed devices which do not have this feature. Divett et al. [20] recently highlighted the potential loss in the annual energy extracted from tidal turbines which operate in non bi-directional currents, and there will also be implications on the device loading.

Three azimuthal angles to the rotor plane are considered in the analysis, ranging from a relatively small and possibly common yaw error of θ=10°, to more severe θ=30°. For these yaw angles the mean longitudinal velocity will be equal to 0.98, and $0.87U_{\theta}$=0° respectively, which will reduce the magnitude of the longitudinal turbulent velocity fluctuations by a corresponding amount. This misalignment will also mean that the longitudinal and lateral turbulence components will both have components in the turbine axial direction, and in the direction of the rotor plane.

D. *Turbulence intensity and length scales*

As for wind turbines, tidal turbine blade loads are considered to be highly sensitive to the turbulence intensity. In the parametric analysis conducted in references [3] and [4] the turbulence intensities analyzed ranged from 5 to 12

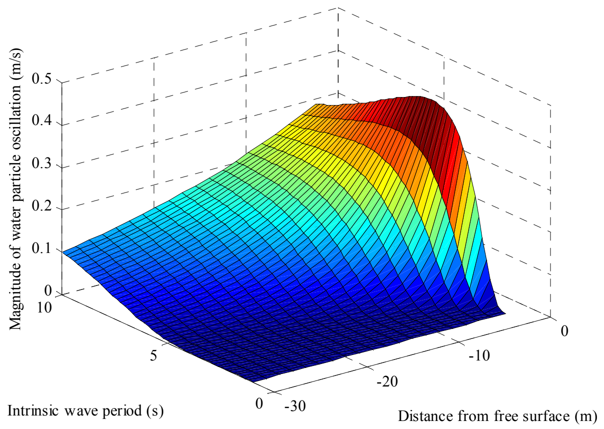

Figure 4. Magnitude of water particle oscillation due to surface waves as a function of intrinsic wave period and distance from the free surface for a 30m deep channel

percent, and approximately 9 to 12 percent respectively, the latter ranges being representative of that measured at hub height for the EMEC site. Noting these ranges, the analyses performed herein consider three longitudinal turbulence intensities: TI_u=7.5%, 10% and 12.5%, where the ratio TI_u:TI_v:TI_w=1:0.8:0.6. To analyze the effect of the lateral and vertical turbulence intensities, the longitudinal turbulence intensity is held constant at 7.5% and TI_v is varied between 6% and 10% whilst TI_w is varied from 4.5% to 7.5%.

As no underwater turbulence spectral model currently exists for these types of sites, the turbulent flow field is synthesized according to the improved von Karman spectrum [21], commonly used for atmospheric turbulence. In the absence of precise measurements of the turbulent flow field structures at a typical tidal turbine site, reference [4] shows reasonable agreement between the synthesized spectrum and the measured data available. With the improved von Karman model the turbulence integral length-scales, as well as being functions of the mean flow speed, are dependent on the roughness length z_0 and, due to Coriolis forces, also the latitude. To avoid independently examining the effect of the nine length scales, ${}^{x}L_{\beta}$, ${}^{y}L_{\beta}$ and ${}^{z}L_{\beta}$ (where β=u,v,w), z_0 was selected as the independent parameter. In all the analyses performed, the latitude was held constant at 50° and the roughness length was varied from $3\text{x}10^{-3}$ m to $3\text{x}10^{-5}$ m. Under these conditions, for mean flow speeds of U_{hub}=1.75m/s and 2.25m/s at a hub height of 15m, the integral length-scale for the longitudinal component of turbulence in the horizontal direction, ${}^{x}L_u$, varies from approximately 28m to 10m and 35m to 14m respectively. These ranges encompass the length-scales proposed by Nezu and Nakagawa [22] for open channel turbulence, in which they use the approximation ${}^{x}L_u \approx 0.8d$.

E. *Wave state and hub height relative to channel depth*

The analyses performed in this paper consider an irregular wave train that is in-line with the rotor axis and traveling in the same direction as the current. As previously stated, the JONSWAP spectral model is utilized in the calculation of the wave kinematics. Two combinations of significant wave height H_s=1m and 2m, and intrinsic peak spectral period T_p=3s and 6s are analyzed, which again from reference [4], are deemed representative of that which is typically observed at the EMEC tidal stream site. Since the severity of the wave induced loads will vary with depth through the water column, the analyses have considered two hub heights z_{hub}=15m and 20m above the seafloor, with the channel depth assumed constant at d=30m.

As a preliminary indication of the likely affect of the waves and hub height, a surface plot of the magnitude of the longitudinal wave particle velocity oscillation is shown in Fig. 4, as given by (6), which is a function of wave period and distance from the free surface,

$$|u(z)| = \frac{H}{2}\omega_i \frac{\cosh\left[k(z+d)\right]}{\sinh(kd)}. \quad (6)$$

For a hub 15m from the free surface; the effect of an intrinsic wave period of 3s is unlikely to be noticeable except possibly by the tips of the rotor as it passes top-dead-center; in contrast to a wave period of 6s where the wave is likely to be felt across the entire rotor plane and therefore induce a noticeable load. For a hub 10m from the free surface; a wave period of 3s is still likely to only affect the rotor as it passes near top-dead-center; whilst for a wave period of 6s the magnitude of oscillations and hence the loading is likely to be much more significant.

V. Relative Effect of Parameters on Fatigue and Extreme Loads

In this section the root-bending moment fatigue and maximum loads for the various cases are compared to provide a preliminary indication of their relative importance. The analyses are performed by varying one parameter at a time, whilst the remaining parameters are held constant at the baseline values stated in Table 1. To reduce the number of simulations, as a first approximation, interaction between the independent parameters is neglected, except for the wave state and hub height interaction. The loads have been computed as averages from multiple ten-minute simulations.

A. *Fatigue loads*

Damage equivalent loads (DELs) are used to equate the damage which would be expected from a variable loading time history to that which would inflicted by a single amplitude sinusoidal load applied at a given frequency. The damage is predicted using Palmgren-Miner linear cumulative damage law [23] and the number of cycles to failure is obtained using a power law representation of the stress-number of cycles (S-N) curve for the material. Although the

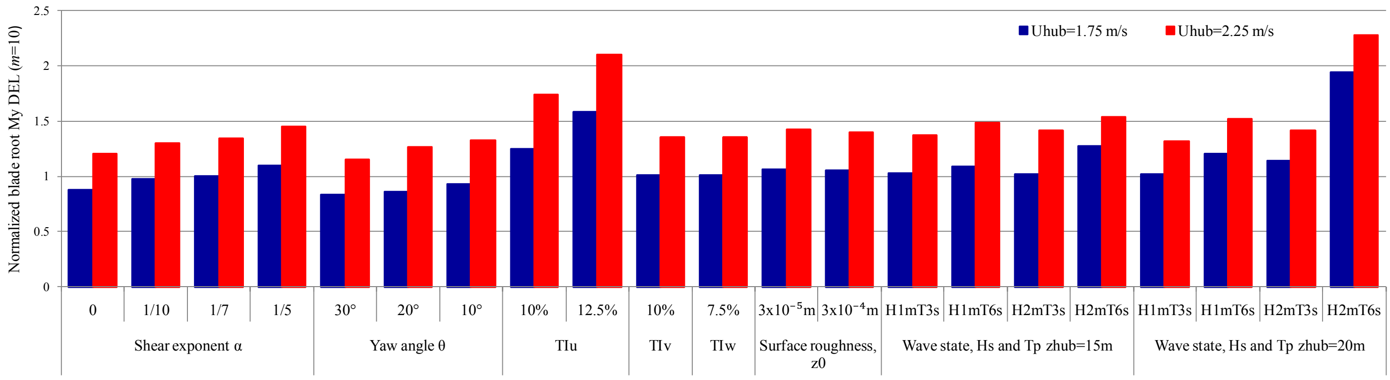

Figure 5. Comparison of blade root M_y fatigue loads for various onset flow parameters

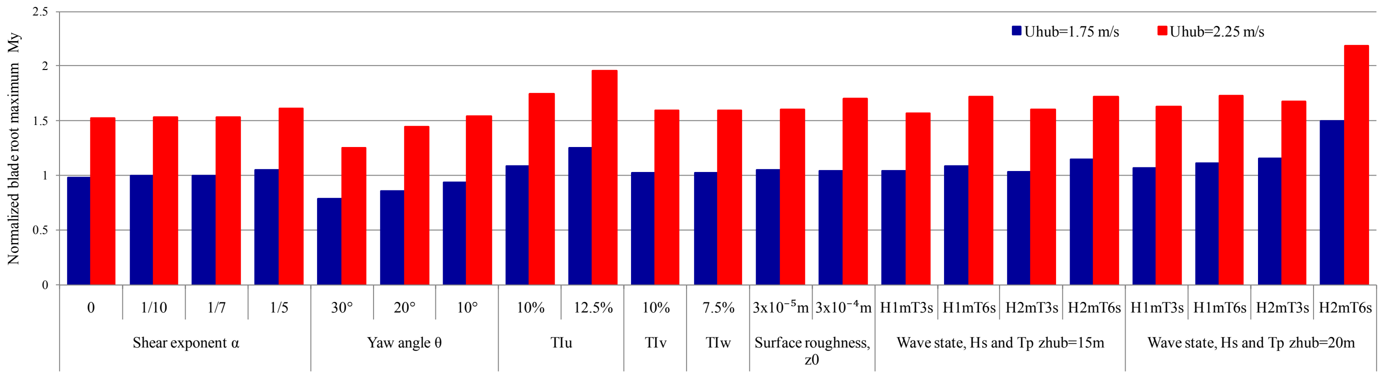

Figure 6. Comparison of blade root M_y maximum loads for various onset flow parameters

power law formulation is independent of the mean stress, it is considered a good first approximation for this analysis. The power law also has the advantage that the DELs can be calculated in terms of load and not stress, such that the root geometry can be neglected. The DEL can be expressed as,

$$DEL = \left[\frac{\sum_i n_i L_i^{\,m}}{Tf} \right]^{1/m}, \tag{7}$$

where m is the slope of the material S-N curve, n_i is the number of cycles at load L_i, which in this case is the root-bending moment, T is the period of time considered and f is the frequency at which the equivalent load is applied.

The comparison of the DELs for various onset flow parameter cases is shown in Fig. 5. The results have been normalized by a load case conforming to a hub height mean current speed of 1.7m/s and the baseline parameters as given in Table 1, for which a 1Hz DEL of 109 kNm is predicted.

The preliminary results indicate that the mean flow velocity, longitudinal turbulence intensity, wave state, and relative height of hub are the primary drivers of the fatigue loads. The vertical shear, yaw angle, lateral and vertical turbulence intensities, and turbulence length scales appear to have only a secondary influence.

The importance of the turbulence intensity agrees with that demonstrated by McCann [3] and McCann et al. [4] and with that which would be expected in the wind turbine industry [24]. In terms of the length scales, while all nine turbulence components were simultaneously varied, their general effect appears to be comparatively minor. In respect to the effect of wave state and hub height, the results correlate well with that inferred from Fig. 4. Waves with a period of 3 seconds are unlikely to penetrate to a sufficient depth to inflict a noticeable load of the blade, whilst waves with periods of 6 seconds will; with the latter effect enhanced when the hub is closer to the surface. As expected, an increase in wave height will increase the velocity perturbation magnitude and hence inflict a greater load.

The relatively low sensitivity of the blade loads to the vertical shear suggests that it is less influential for tidal turbine loads than for wind turbine loads, where it is typically considered to be an important parameter. However, this could possibly be explained by the considerable difference in rotor diameters between a tidal turbine and a modern-wind turbine, the latter which typically has a diameter exceeding 60 m. In terms of the effect of yaw, since angles exceeding 30° are expected to be rare, it may also be concluded that a slight yaw angle in the order of 10° will generally be insignificant in terms of both fatigue and extreme loading.

TABLE I
BASELINE FLOW FIELD

α	1/7
θ	0°
TI_u:TI_v:TI_w	7.5:6:4.5 %
z_0	$3\text{x}10^{-3}$ m
z_{hub}	15m
H_s, T_p	0,0

B. *Maximum loads*

The comparison of the maximum loads for various onset flow parameter cases is shown in Fig. 6. The results have also been normalized by the same simulation case as above, for which a maximum load of 238 kNm is predicted.

Similar trends as for the fatigue loads can be observed, with the mean flow speed, longitudinal turbulence intensity, wave action, and hub height having the most significant affect. However the effect of the shear exponent, appears to less pronounced than for fatigue, whereas the effect of yaw error is more significant.

VI. COMPARISON OF LOAD DISTRIBUTIONS

The Rainflow cycle counted load distributions have been analyzed as a means of explaining the relative effect of the various inflow parameters on the DELs. As previously stated, although the mean load will likely have an influence on the blade fatigue, the form of the DEL expressed by (7) is a function of load range only. Hence only the range distribution has been analyzed.

The root out-of-plane bending moment range count distribution, for two cases of mean hub height velocity, are compared in Fig. 7(a). It can be observed that the magnitudes of the low cycle, high load portion are increased with increase in velocity. Similar trends can be noted for cases where the turbulence intensity is increased, as shown in Fig. 7(b). In contrast there is a relatively small change in the high load portion for a change in vertical shear profile exponent, as is depicted in Fig. 7(c).

To identify which features of load distribution have an effect on the DELs, the variable $n_i L_i^m$ has been computed. Its cumulative value, as a function of cycle range for the case of varying velocity, is shown in Fig. 8. For fiberglass composites with m=10, the low cycle, high load portion dominates. Hence the high load region is the primarily driver of the DEL, with the main body of the range distribution having comparatively little contribution. The importance of the low frequency, high-load region for materials with high S-N slope exponents was discussed by Sutherland [24] in the wind turbine fatigue context. It is this part of the tidal turbine blade load spectrum to which significant attention should therefore be directed. This explains why the DELs are so much more sensitive that the maximum loads to variations in mean velocity, turbulence intensity, wave state and hub height, since compared to, e.g. the shear exponent, there is a relatively greater change in the low cycle, high-load region of the curve by the former group of parameters.

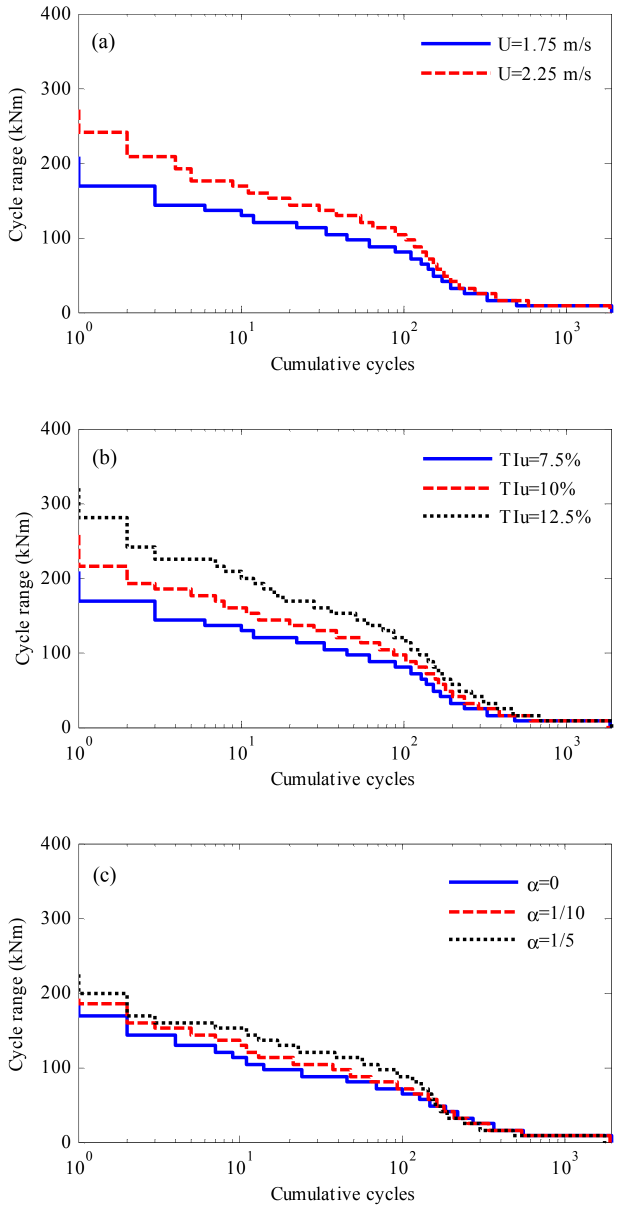

Figure 7. Blade root M_y range count distributions as a function of: (a) U_{hub} (b) TI_u (c) α

VII. LIFETIME FATIGUE DAMAGE ANALYSIS

The results so far have indicated that the mean flow speed is a dominant driver of the blade loads. However, the relative percentage of time that the turbine will be exposed to each mean flow speed may also have an influence. The variation in mean tidal flow is predicted from a model previously used by Fraenkel [25] and Nicholls-Lee and Turnock [26], which combines a spring-neap, or lunar cycle (T_0=353 hr) and a diurnal cycle (T_1=12.5 hr). Combining the model with the

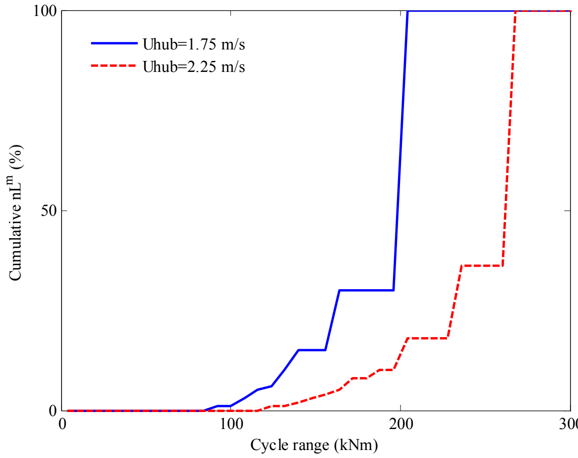

Figure 8. Blade root M_y cumulative $n_iL_i^m$ as a function of U_{hub}

power law shear profile, the hub-height mean velocity can be expressed as,

$$U_{hub}(t) = \left[\left[K_0 + K_1 \cos\left(\frac{2\pi t}{T_0}\right)\right]\cos\left(\frac{2\pi t}{T_1}\right)\right] \cdot \left[\frac{z_{hub}}{d}\right]^{\alpha} \quad (8)$$

The parameters $K_0=\frac{U_s+U_n}{2}$ and $K_1=\frac{U_s-U_n}{2}$, where U_s and U_n are the spring and neap tidal velocities respectively.

For this analysis, four hub height flow speeds: U_{hub}=1.5m/s, 1.75m/s, 2.00m/s and 2.25m/s have been considered, again with the background flow parameters as given in Table 1. The proportion of hours that these speeds are experienced over a spring-neap cycle are computed using (8) and are shown in Fig. 9, for four combinations of U_s and U_n.

The relative effect of the velocity distribution on the loads has been analyzed in terms of lifetime DELs. The Rainflow cycle counted range distribution counts are weighted by the probability of occurrence of the time each mean flow speed is experienced, i.e. $n_i=[n_{U,i}T_U/T_{total}]$, where T_U is the duration of time in which the particular flow speed is experienced and T_{total} is the total duration of time considered.

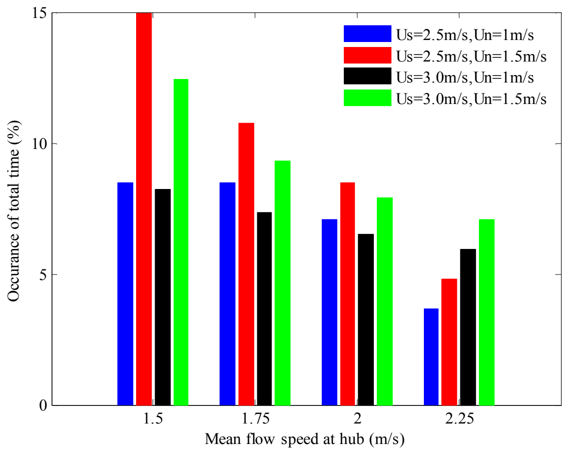

Figure 9. Mean hub-height velocity distribution, as a function of spring and neap currents

TABLE II
EFFECT OF THE MEAN FLOW DISTRIBUTION ON DELS

Site characteristics	Normalized DEL
U_s=2.5 m/s, U_n=1.0 m/s	1
U_s=2.5 m/s, U_n=1.5 m/s	1.03
U_s=3.0 m/s, U_n=1.0 m/s	1.03
U_s=3.0 m/s, U_n=1.5 m/s	1.05

The DELs for the four cases are presented in Table 2, which have been normalized by the DEL for U_s=2.5m/s and U_n=1.0m/s. Whilst above-rated conditions have not been considered, the results suggest that the mean flow distribution has a relatively minor affect on the fatigue loads.

VIII. CONCLUSIONS

The results of the preliminary sensitivity analysis suggest that horizontal mean flow speed, longitudinal turbulence intensity, wave state and relative height of hub compared to channel depth are the most dominant parameters influencing the blade root fatigue and maximum loads. They therefore should be accurately modeled in a loads assessment.

In terms of understanding the fatigue loads, these dominant parameters tend to produce the greatest increase in the magnitudes of the loads in the high load, low cycle portion of the loading distribution. Like composite wind turbine blades, it is this region which, although it has a relatively low occurrence, contributes a disproportionately high amount to the fatigue damage.

The mean velocity distribution appears to have a relatively minor influence on the blade load lifetime damage. However, the analysis has not considered mean flow speeds above rated, which would result in increased loading.

ACKNOWLEDGMENT

I.A.M acknowledges the financial assistance provided by the New Zealand Tertiary Education Commission for this PhD research. The use of *Tidal Bladed* by Garrad Hassan and Partners, and the blade specifications from Tidal Generation Limited and Aviation Enterprises Limited [27] is also gratefully acknowledged.

REFERENCES

[1] F. O Rourke, F. Boyle, and A. Reynolds, "Tidal energy update 2009," *Applied Energy,* vol. 87, pp. 398-409.

[2] G. Marsh, "Wave and tidal power -- an emerging new market for composites," *Reinforced Plastics,* vol. 53, pp. 20-24, 2009.

[3] G. N. McCann, "Tidal current turbine fatigue loading sensitivity to waves and turbulence-a parametric study," in *7th European Wave and Tidal Energy Conference* Porto, Portugal, 2007.

[4] G. McCann, M. Thomson, and S. Hitchcock, "Implications of Site-Specific Conditions on the Prediction of Loading and Power Performance of a Tidal Stream Device," in *2nd International Conference on Ocean Energy* Brest, France, 2008.

[5] "European Marine Energy Centre, " Orkney, UK, www.emec.org.uk.

[6] N. Barltrop, K. S. Varyani, A. Grant, D. Clelland, and X. Pham, "Wave-current interactions in marine current turbines," *Proceedings of the Institution of Mechanical Engineers -- Part M -- Journal of Engineering for the Maritime Environment,* vol. 220, pp. 195-203, 2006.
[7] E. A. Bossanyi, "GH Tidal Bladed Theory Manual," Garrad Hassan and Partners Limited 2008.
[8] A. S. Bahaj, W. M. J. Batten, and G. McCann, "Experimental verifications of numerical predictions for the hydrodynamic performance of horizontal axis marine current turbines," *Renewable Energy,* vol. 32, pp. 2479-2490, 2007.
[9] L. Pitt and D. A. Peters, "Theoretical prediction of dynamic inflow derivatives," *Vertica,* vol. 5, 1981.
[10] ISO, *Petroleum and natural gas industries- Specific requirements for offshore structures- Part 1: Metocean design and operating considerations*, First Edition ed. vol. ISO 19901-1: ISO, 2005.
[11] Y. Goda, "A review on statistical interpolation of wave data," Port and Harbour Research Institute 1979.
[12] C. K. Morooka and I. H. Yokoo, "Numerical simulation and spectral analysis of irregular sea waves," *International Journal of Offshore and Polar Engineering,* vol. 7, pp. 189–196, 1997.
[13] J. D. Wheeler, "Method for Calculating Forces Produced by Irregular Waves," *Journal Of Petroleum Technology,* vol. 22, pp. 473-486, 1970.
[14] "Tidal Generation Limited," Bristol, UK, www.tidalgeneration.co.uk.
[15] P. Fraenkel, "Marine current turbines: pioneering the development of marine kinetic energy converters," *Proceedings of the Institution of Mechanical Engineers, Part A: Journal of Power and Energy,* vol. 221, pp. 159-169, 2007.
[16] L. Myers, "Operational parameters of horizontal axis marine current turbines," Ph.D. dissertation, University of Southampton, Southampton 2005.
[17] M. Drela, "XFoil: an analysis and design system for low Reynolds number airfoils," in *Conference on Low Reynolds Number Airfoil Aerodynamics* University of Notre Dame, Indiana, 1989.
[18] A. F. Molland, A. S. Bahaj, J. R. Chaplin, and W. M. J. Batten, "Measurements and predictions of forces, pressures and cavitation on 2-D sections suitable for marine current turbines," *Proceedings of the Institution of Mechanical Engineers, Part M: Journal of Engineering for the Maritime Environment,* vol. 218, pp. 127-138, 2004.
[19] R. F. Nicholls-Lee and S. R. Turnock, "Enhancing Performance of a Horizontal Axis Tidal Turbine using Adaptive Blades," in *OCEANS 2007 - Europe*, 2007, pp. 1-6.
[20] T. Divett, R. Vennell, and C. Stevens, "Maximising energy capture by fixed orientation tidal stream turbines in time-varying off axis current," in *Australasian Coasts and Ports Conference*, Wellington, New Zealand, 2009, pp. 1-6.
[21] ESDU, *Characteristics of atmospheric turbulence near the ground. Part II: Single point data for strong winds (neutral atmosphere)*: EDSU 85020. Engineering Sciences Data Unit, UK, 1985 (amended 1993).
[22] I. Nezu and H. Nakagawa, *Turbulence in Open-Channel Flows*: A.A.Balkema, 1993.
[23] M. A. Miner, "Cumulative damage in fatigue," *Transactions of the American Society of mechanical Engineers,* vol. 67, pp. A159-A164, 1945.
[24] H. Sutherland, "On the fatigue analysis of wind turbines," Sandia National Laboratories, Albuquerque, New Mexico 1999.
[25] P. L. Fraenkel, "Power from marine currents," *Proceedings of the Institution of Mechanical Engineers, Part A: Journal of Power and Energy,* vol. 216, pp. 1-14, 2002.
[26] R. F. Nicholls-Lee, S. R. Turnock, and S. W. Boyd, "Performance prediction of a free stream tidal turbine with composite bend-twist coupled blades," in *2nd International Conference on Ocean Energy* Brest, France, 2008.
[27] "Aviation Enterprises Limited," Lambourn, UK, www.aviationenterprises.co.uk.